Vol. 498: 85–94, 2014
doi: 10.3354/meps10611

MARINE ECOLOGY PROGRESS SERIES
Mar Ecol Prog Ser

Published February 17

Influence of buried *Ulva lactuca* on denitrification in permeable sediments

Michael F. Bourke, Adam J. Kessler, Perran L. M. Cook*

Water Studies Centre, Monash University, Clayton, Victoria 3800, Australia

ABSTRACT: Macroalgae can form extensive blooms in coastal areas receiving high nitrogen loading, and a large fraction of this biomass is likely to be degraded in permeable sediments. We undertook a series of experiments investigating the influence of buried macroalgae *Ulva lactuca* on denitrification in permeable sediments using flow-through reactor and flume experiments. Our results showed that in flow-through chamber experiments, the presence of buried macroalgae generally did not enhance rates of denitrification, although an enhancement of coupled nitrification–denitrification was observed at intermediate porewater flow rates. 2D planar optode images revealed that leaching dissolved organic carbon (DOC) from buried macroalgal sheets resulted in a plume of hypoxic-anoxic sediment that had only a very small stimulating influence on denitrification rates (observed rates range from 0.1 to 3 µmol m^{-2} h^{-1}). Flume experiments showed that buried macroalgae sheets had a pronounced effect on porewater flow fields within the sediment, and that the effect on denitrification was highly dependent upon the position of the buried macroalgae relative to ripple geometry. Overall, our results showed that rates of denitrification were orders of magnitude lower in flume experiments with realistic flow fields compared to column experiments with artificial flow fields, in agreement with previous work. We conclude that the presence of buried macroalgae does not significantly stimulate denitrification rates within permeable silicate sands.

KEY WORDS: *Ulva lactuca* · Denitrification · Permeable sediments · Anoxic plume · Advection

INTRODUCTION

Eutrophication is an increasing problem globally and results primarily from excess nitrogen inputs in coastal waters (Conley et al. 2009). The major sink for bioavailable nitrogen in coastal sediments is denitrification, whereby nitrate (NO_3^-) is used as a terminal electron acceptor and is in turn reduced to N_2 gas. The process requires anoxic conditions, an electron donor (organic matter) and a source of NO_3^-. Within sediments, NO_3^- may be sourced from the water column (termed uncoupled denitrification) or produced via the oxidation of NH_4^+ within the oxic zone of the sediment (termed coupled denitrification). Given its ecological importance, denitrification has been extensively studied; however, the vast majority of studies have taken place within cohesive (muddy) sediments. The few studies that have taken place within permeable sediments (e.g. Seitzinger & Giblin 1996) have used conventional chamber approaches, which are unlikely to give realistic rate measurements because chamber emplacement changes the porewater flow fields within the sediment which control the denitrification rate and transport of N_2 out of the sediment (Cook et al. 2006).

Permeable sediments cover 70% of the continental shelf and dominate coastal areas (Emery 1968), and have previously been overlooked in biogeochemical studies (Boudreau et al. 2001), although permeable sediment research is now rapidly expanding. Advective porewater flow-through permeable sediments can dominate solute transport and has a marked

*Corresponding author: perran.cook@monash.edu

impact on biogeochemical processes, which needs to be taken into account when designing experiments to measure process rates (Huettel et al. 2003, Cook & Røy 2006, Cook et al. 2006). Recent studies on denitrification in permeable sediments have shown that this process is strongly controlled by porewater flow rates; however, the significance of this process in permeable sediments remains under debate, with some studies suggesting high rates (Rao et al. 2008, Gihring et al. 2010, Santos et al. 2012) of denitrification and others suggesting much lower rates (Cardenas et al. 2008, Kessler et al. 2012).

Macroalgae are a particularly conspicuous consequence of eutrophication, with significant growth of species such as *Ulva lactuca* being observed around the world (Guinda et al. 2012, Tabarsa et al. 2012). This algal biomass represents a significant source of organic carbon and nitrogen that can be degraded both within the sediment and the water column (Hardison et al. 2010). Macroalgae may affect denitrification in a number of ways. Increased organic matter and nitrogen inputs may stimulate denitrification (McMillan et al. 2010, Eyre et al. 2011). Conversely, assimilation of nitrate by macroalgae has been shown to decrease denitrification (Dalsgaard 2003). Of key importance, it has been shown that the proportion of nitrogen removed via denitrification (denitrification efficiency) decreases as organic matter loading increases (Eyre & Ferguson 2009). Consistent with this, it has been shown that in systems with a high accumulation of transient macroalgae such as *U. lactuca*, very little of the nitrogen released from macroalgal biomass is denitrified relative to inorganic nitrogen released (Trimmer et al. 2000). It has also been suggested that dissimilatory nitrate reduction to ammonium (DNRA) will begin to dominate over denitrification leading to a feedback loop of enhanced eutrophication (McGlathery et al. 2007). As such, macroalgae undergoing degradation within cohesive (muddy) sediments are likely to be a significant source of bio-available nitrogen back to the water column.

There have been no studies on the effect of buried macroalgae on denitrification within permeable sediments. It is likely that the presence of such material could increase denitrification in permeable sediments through a number mechanisms: (1) Dissolved organic carbon (DOC) released from the macroalgae enhances oxygen consumption within the sediment leading to anoxic hotspots (Franke et al. 2006) in which denitrification can take place. (2) DOC released from the macroalgae will provide additional electron donors to fuel denitrification within the anoxic zones of the sediment. (3) Ammonium released from the macroalgae may undergo nitrification with the sediment, increasing NO_3^- availability. (4) The physical obstruction of the flow field by algal detritus may enhance the occurrence of anoxic zones within the sediment.

This study set out to mechanistically investigate the plausibility of these mechanisms and, in particular, the extent to which macroalgal detritus alters oxygen penetration dynamics and the effect this has on denitrification. We investigated this using a combination of flow-through column and flume experiments with simultaneous quantification of denitrification and oxygen dynamics using planar optodes.

MATERIALS AND METHODS

Study site and sample collection

Sediment and seawater samples were collected at Middle Park beach (–37.848° S, 144.948° E) located on the eastern shore of Port Phillip Bay in Victoria, Australia. The sediment had a permeability of 8.3×10^{-12} m^2 and a porosity of 0.53 measured using a constant head permeameter (Reynolds 2008) and drying saturated samples respectively. The top 5 cm of sediment was collected approximately 5 m from the shoreline at low tide. Additionally, about 120 l of seawater was collected using plastic carboys which were cleaned and rinsed prior to collection. Within 1 h of collection, the samples were transported to Monash University, where the overlying water was bubbled with air using an aquarium air stone in order to maintain oxic conditions at the sediment surface. Samples of *Ulva lactuca* were collected, washed with seawater and frozen — which would have led to the lysis of algal cells, and so the experiments presented here represent the algae at its most labile. Sample collection was performed on 3 occasions (15 Apr 2011, 30 Sep 2011 and 01 Apr 2012) for the cylindrical column experiments, the planar optode flow-through chamber experiments and the flume experiments, respectively.

Ulva lactuca denitrification experiments

Six cylindrical flow through columns (4.6 cm diameter, 10 cm length) as described by Evrard et al. (2013) were packed with sieved sediment. In 3 of these columns, 1 cm^2 sheets of *Ulva lactuca* were cut and placed in the center of the column and perpendicular to the flow 25, 40, 55 and 70 mm from the column

inlet. The remaining 3 columns served as the control columns that had no *U. lactuca* sheets embedded within the sediments. Breakthrough curves showed this column set-up exhibited plug flow as shown in Evrard et al. (2013). Dissolved oxygen at the column outlets was monitored using a Hach HQ40d LDO probe inserted into a custom-built flow-through cell.

The reservoir was aerated for the duration of the experiments. The chambers were left to equilibrate over a 3 d period at the maximum flow velocity studied (36.2 cm h^{-1}). Following this period, the inlet reservoir was amended with $^{15}NO_3^-$ (50 µmol l^{-1}) and left for 2 residence times before any measurements commenced (based on our observations of $^{29}N_2$, $^{30}N_2$ and O_2 behavior, which typically stabilizes after 2 residence times). The sampling procedure involved attaching glass syringes to each of the effluent lines and collecting nutrient and N_2 samples at each flow velocity. Once collected, the flow velocity was reduced and the chambers were left to equilibrate for a minimum of 2 residence times, and the sampling regime was repeated. Samples were collected at each of the following flow velocities: 2.38, 4.22, 8.11, 15.8 and 36.2 cm h^{-1} and are within the range previously reported for porewater advection in the surface of permeable sediments (Precht et al. 2004). This corresponds to residence times of approximately 20 min to 3 h.

Planar optode flow-through chamber experiments

A rectangular flow-through cell was constructed from 5 mm thick acrylic (70 mm wide × 30 mm deep × 43 mm high) to allow the emplacement of a 2D planar optode foil to determine oxygen concentration within the chamber (Larsen et al. 2011) (Fig. 1). Rhodamine dye tracer experiments were undertaken to confirm that plug flow was achieved when water was pumped through the top end cap of the column, with a 5 mm gap between the inlet cap and the sediment water interface and to visualize the effect on the flow dynamics in the presence of a 1 cm wide, 35 mm long plastic obstruction (same size as the *Ulva lactuca* piece, see below).

On 21 Nov 2011, the column was prepared by submerging the chamber in a bucket of sample seawater and gradually filled with sieved (2 mm mesh) sample sediment. A sheet of *Ulva lactuca* (10 × 35 mm) was placed in the centre of the sand bed, perpendicular to the chamber's lengths so that the edges of the *U. lactuca* were in contact with the chamber wall and the planar optode. Another 8 mm of sample sand was

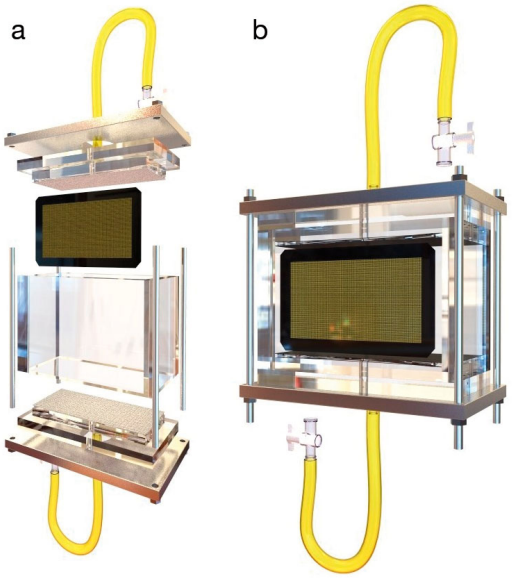

Fig. 1. Rendering of optode flow-through chamber: (a) exploded view, (b) collapsed view. Inlet and outlet caps are overlaid with fine mesh, positioned in line with rectangular acrylic body. Chamber is housed in a metallic clamp

placed in the chamber and the inlet cap was connected, leaving 5 mm between the sediment water interface and the inlet cap. Finally, the sediment was gently compacted by rocking the chamber from side to side, which helped produce even plug flow. The chamber was then attached to a peristaltic pump with oxygen sensors at the inlet and outlet of the column (Pyroscience flow-through cells, attached to a Firesting 4 channel optical dissolved oxygen sensor). Water was pumped into the chamber from a reservoir containing filtered and aerated seawater and allowed to recirculate. This procedure was carried out carefully ensuring that the inlet lines were submerged so that bubbles were prevented from entering the chambers. The column was maintained for 9 d, during which 4 experiments were undertaken as detailed in Table 1 (Expts E1 to E4).

For each experiment, the starting flow velocity was set to the minimum rate at which the column was entirely oxic (>150 µmol l^{-1}), which was determined using the outlet O_2 sensors. The experiment progressed by capturing images of the planar optode and taking samples for labeled N_2 and nutrients after the oxygen concentration at the outlet had stabilized (>2 residence times). Experiments were run from high to low flow velocities (minimum and maximum flow velocities presented in Table 1) to prevent the accumulation of reduced solutes, which would lead to additional O_2 consumption. During chamber experiments, the background oxygen consumption rate

Table 1. Isotope pairing experiments performed using the planar optode flow-through chamber

Experiment	Date	Flow velocity (cm h^{-1})	
		Maximum	Minimum
E1	23 Nov 2011	8.16	3.92
E2	25 Nov 2011	16.57	6.04
E3	28 Nov 2011	31.36	10.02
E4	29 Nov 2011	22.92	8.15

increased, most likely due to changes in the microbial community in the sand as has previously been observed (Kessler et al. 2012), and/or owing to the buildup of DOC in the reservoir from decaying macroalgae. Each experiment commenced with the reservoir being amended with $^{15}NO_3^-$ to a final concentration of 20 µmol l^{-1} (~1 µmol l^{-1} $^{14}NO_3^-$ background). Samples for N_2 and nutrients were taken from the column outlet using a glass syringe attached directly to the outlet line.

Flume experiments

A recirculating flume tank was used to simultaneously measure 2D oxygen distribution using a planar optode and isotopically labeled N_2 throughout the sediment as previously described (Kessler et al. 2012). Previous work has shown that there is a negligible release of labeled N_2 from the sediment over the timescale of the experiment, thus negating the need for a sealed flume (Kessler et al. 2012). The flume was filled with sieved sediment (2 mm mesh sieve) and ripples sculpted with a wavelength of 10 cm and a height of 1.5 cm.

Prior to the experimental setup, two 1.5 × 11 cm sheets of *Ulva lactuca* were prepared by overlaying 5 sheets. These sheets were flattened and frozen within a plastic bag and cut so their length and width were uniform. Two flume denitrification experiments were performed: one with the sheets midway between the ripple peak and trough at approximately 45°(Expt F1) and one with the sheets laid flat at the base of the sediment ripple trough (Expt F2). These positions were selected as they represent locations with high rates of porewater advection into the sediment.

In order to embed the *Ulva lactuca* in the sediment, the sheets were sandwiched between 2 layers of plastic, which were removed after burial. This procedure was necessary to prevent the *U. lactuca* sheet separating as it was submerged. The overlying flow velocity was set to approximately 16 cm s^{-1} and the flume was left to equilibrate for 3 d. Prior to tracer addition (final $^{15}NO_3^-$ concentration of 50 µmol l^{-1}), nutrient and N_2 samples were taken from the water column. A second water sample was taken for nutrient analysis 10 min after tracer addition to determine the $^{15}N/^{14}N$ ratio at $t = 0$.

Optode images were taken every 15 min throughout the incubation to track sediment oxygen dynamics. After 24 h of incubation, 3 ml porewater samples were collected from silicon ports using a 10 cm needle that had holes drilled in the side at 5 mm intervals to ensure a cylinder of water was sampled across the width of the flume. The sediment was then stirred to form a slurry, and the flume turned on for 10 min to mix the water column, after which another set of nutrient and N_2 samples were taken.

Sample preservation and analysis

Nutrient samples were filtered through a 0.45 µm filter (MicroAnalytix 30PS045AN) and frozen; N_2 samples were taken in 3 ml Exetainers (Labco) and preserved with 250 µl of 50% (w/v) $ZnCl_2$. The N_2 samples taken in the cylindrical flow-through chamber experiments were analyzed using the coupled gas chromatograph-mass spectrometer (Shimazu GCMS-QP5050) whilst the flow-through chamber and flume samples were analyzed using a Sercon 20-22 isotope ratio mass spectrometer coupled to a gas chromatograph. Combined nitrate and nitrite (NO_x) were analyzed spectrophotometrically using a Lachat QuikChem 8000 Flow Injection Analyzer (FIA). Areal rates of $^{29}N_2$ and $^{30}N_2$ production were calculated by multiplying the measured excess of $^{29}N_2$ and $^{30}N_2$ by the flow rate through the column divided by the cross sectional area of the column. Rates of $^{14}NO_3^-$ and $^{15}NO_3^-$ reduction (D_{14} and D_{15}, µmol m^{-2} h^{-1}) were calculated using the isotope pairing equations (Nielsen 1992).

RESULTS

Cylindrical column experiments

D_{14} rates were generally very low in the cylindrical column experiments, reflecting the extremely low NO_x concentrations in the water reservoir and lack of nitrification (Fig. 2). Effluent was anoxic for all cases except at 36.2 cm h^{-1}. Mean effluent oxygen concentrations at 36.2 cm h^{-1} were 118 µmol l^{-1} in the *Ulva lactuca* columns and 128 µmol l^{-1} in the control

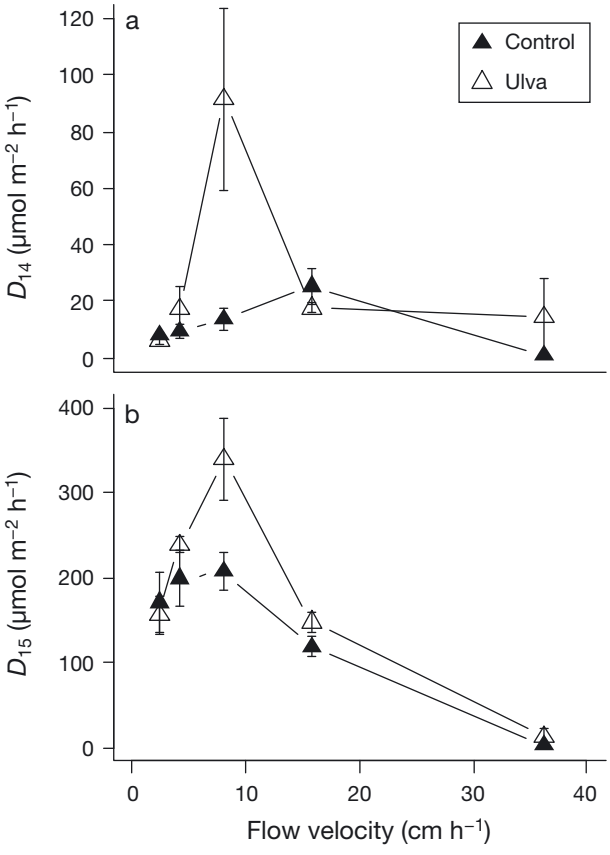

Fig. 2. Rates of denitrification (mean ± SE, n = 3) of $^{14}NO_3^-$ and $^{15}NO_3^-$ (µmol m^{-2} h^{-1}) at varying flow rates during cylindrical column experiments

columns. D_{14} increased slightly at flow velocities >4.22 cm h^{-1}, from 9.51 to 25.4 µmol m^{-2} h^{-1}. There was little difference in the rates between the *U. lactuca* and control columns with the exception of the flow rate of 8.11 cm h^{-1} for which the *U. lactuca* treatment had a marked and significant spike in D_{14} up to 91.5 µmol m^{-2} h^{-1} (1-way ANOVA, $p < 0.05$). Rates of D_{15} were an order of magnitude higher than D_{14}, reflecting the higher concentrations of $^{15}NO_3^-$, in the water reservoir (50 µmol l^{-1} cf. 1 µmol l^{-1}). D_{15} peaked at 8.11 cm h^{-1} for both treatments. The rates of D_{15} were not significantly different from one another with the exception of a flow rate of 8.11 cm h^{-1} when D_{15} was 215 µmol m^{-2} h^{-1} and 340 µmol m^{-2} h^{-1} in the control and *U. lactuca* treatments, respectively ($p < 0.05$, 1-way ANOVA).

Planar optode flow-through chamber experiments

Dye tracer experiments showed that an even plug flow through the column was achieved, and that the presence of a plastic obstruction had no noticeable effect on the evenness of the dye front (Fig. 3). Optode images revealed that at a flow velocity of 10 cm h^{-1} the column sediment was highly oxic with 98.2% of the column having an oxygen concentration >125 µmol l^{-1}. Over the following days, a plume of lower oxygen concentration developed downstream of the *Ulva lactuca* pieces (Figs. 4 & 5). Throughout each of the 4 flow-through chamber experiments, the same pattern of oxygen depletion was observed. Across the 4 experiments (Expts E1 to E 4), denitrification rates only began to increase once effluent porewater became anoxic, after which rates increased rapidly to ~50 µmol m^{-2} h^{-1} (Fig. 6).

Flume experiments

The sequence of planar optode images revealed that there was a steady state maintained during the experiment, with very little variation in the oxygen penetration dynamics over time (data not shown). Fig. 7 depicts an anoxic plume at the third ripple stemming from the position of the embedded *Ulva lactuca* in Expt F1. The plume is curved upwards toward the sediment ripple crest, which is indicative of the porewater advective flow paths. This pattern was not observed in the first sediment ripple, which

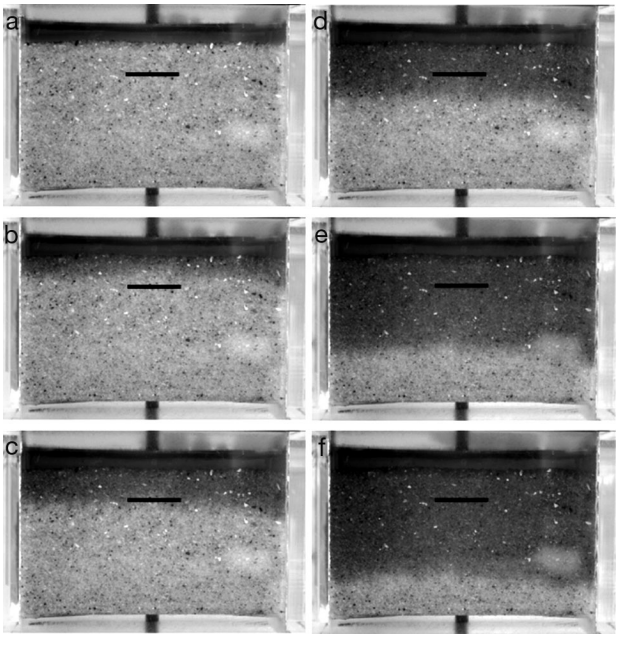

Fig. 3. Rhodamine dye front moving through the flow-through chamber in the presence of a piece of plastic (marked with the horizontal black line). Flow rate was 1.1 ml min^{-1} or ~10 cm h^{-1}; images shown were taken at (a) 0, (b) 4.17, (c) 7.5, (d) 11.42, (e) 19.17 and (f) 22.09 min. The mark on the lower right of the images is flash glint

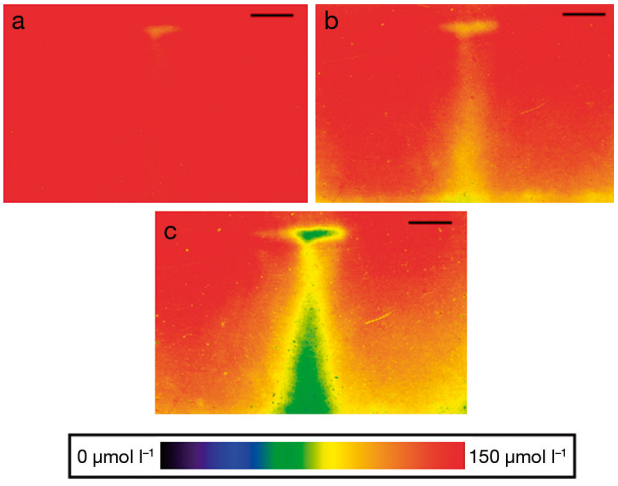

Fig. 4. Planar optode images depicting gradual formation of a plume of lower oxygen concentration. All images were captured whilst the system was operating at a flow velocity of approximately 8 cm h^{-1}. Black scale bar indicates a length of 5 mm. Images (a), (b) and (c) correspond to images taken on the same day, the first and second day after *Ulva lactuca* addition, respectively

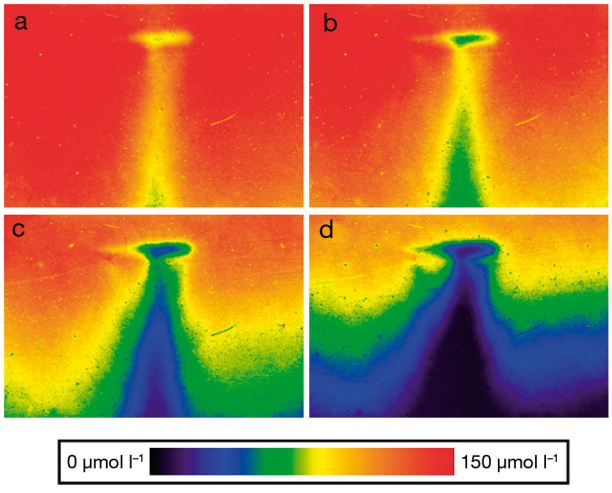

Fig. 5. Planar optode images during box chamber Expt 1 (2 d after *Ulva lactuca* emplacement) at gradually reducing flow velocities. Images (a), (b), (c) and (d) were captured at flow velocity = 8.16, 7.99, 7.02 and 5.96 cm h^{-1}, respectively

also has the *U. lactuca* embedded in a similar position. The most likely explanation for this inconsistency is that the *U. lactuca* was not placed correctly in the first sediment ripple, resulting in oxic water passing between the sheet and the optode. Fig. 7 shows that beneath the obstructed ripples (1st and 3rd) there is deeper oxygen penetration into the sediment compared to the control ripples with a depth difference of 2.5 cm. Fig. 7 also indicates that there is no clear difference between the oxygen penetration dynamics between sediment ripples with or without obstruction in Expt F2. The denitrification rates determined from the sediment slurry in flume Expts F1 and F2 were 3.78 and 5.03 µmol m^{-2} h^{-1}, respectively. The concentrations of $^{29}N_2$ and $^{30}N_2$ detected in the sampling regions in the 2 flume experiments are shown in Figs. S1 & S2 in the Supplement at www.int-res.com/articles/suppl/m498p085_supp.pdf.

DISCUSSION

Column experiments

We hypothesized that the addition of *Ulva lactuca* obstructions to the sediment would create hotspots within permeable sediments, and that these would lead to a stimulation of denitrification through the supply of labile organic carbon and anoxia created by increased respiration, and possibly porewater flow 'dead zones' induced by flow obstruction. The 3 experiments undertaken here, however, suggest that *U. lactuca* had a very limited effect on denitrification rates through this mechanism. In the first experiment, there was no significant difference between D_{15} in the cores with and without *U. lactuca,* with the exception of a flow rate of 8.11 cm h^{-1}, when there was a small (factor 1.5) significant increase (Fig. 2). The water flowing out of these columns was anoxic at flow rates at and below 15.8 cm h^{-1}, and the similarity between the denitrification rates in the 2 treatments under these conditions suggests that the addition of organic carbon did not stimulate denitrification on the time scale of hours. At a flow rate of 36.2 cm h^{-1}, the column effluent was oxic, and there was no significant difference between the rates of denitrification in the 2 treatments, suggesting that the creation of anoxic microsites (if any) by the macroalgae did not stimulate denitrification.

There was a statistically significant stimulation of denitrification at a flow rate of 8.11 cm h^{-1}, where D_{14} increased by a factor of 6 from 14 to 91.5 µmol m^{-2} h^{-1}. This was driven by a spike in coupled nitrification–denitrification, which is most likely explained by the release of NH_4^+ from *Ulva lactuca,* which was subsequently nitrified in the oxic zone of the column before being denitrified in the anoxic zone. The change in the importance of D_{14} with flow is explained as follows: at low flow rates, the columns are mostly anoxic, so little nitrification of the NH_4^+ released from *U. lactuca* takes place. As flow rates increase, the oxic volume of the column increases, increasing the rate of nitrification, and subsequent denitrification in the anoxic portion of the column. A further increase in the

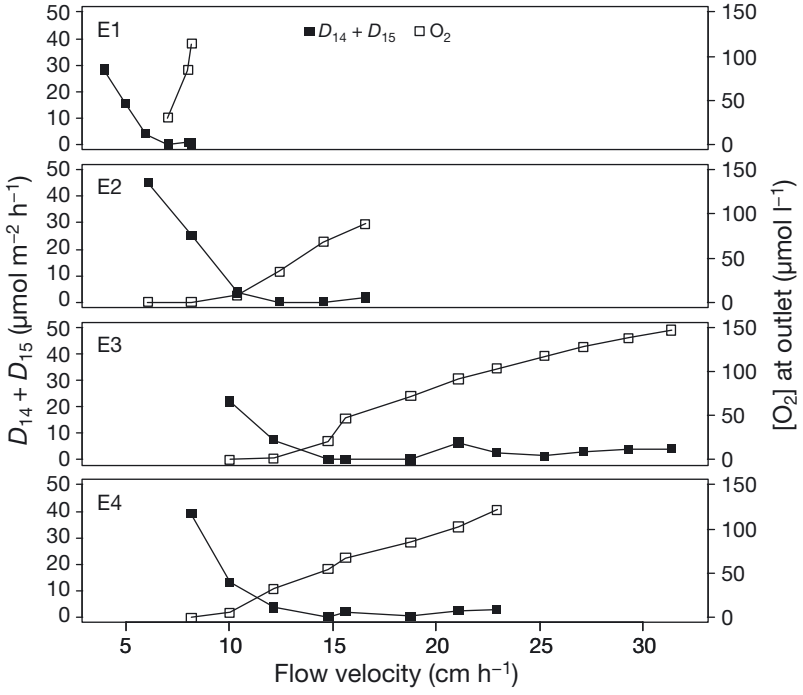

Fig. 6. Total denitrification rate of $^{14}NO_3^-$ and $^{15}NO_3^-$ (D_{14} + D_{15}) and outlet O_2 concentration versus flow velocity for Expts E1, E2, E3, and E4

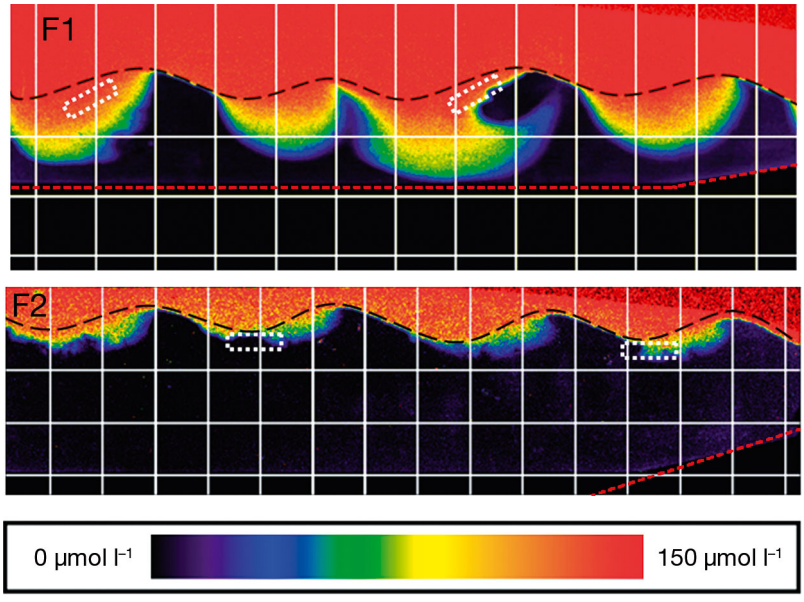

Fig. 7. Planar optode images from flume experiments 1 and 2 (F1 and F2). Vertices of lines indicate sampling port positions. Dashed black lines indicate the sediment water interface. Dashed red line marks the edges of the planar optode. The sediment below the dashed red line was unobserved but can be assumed to be anoxic. Dashed white line boxes mark the positions of the *Ulva lactuca* pieces. The direction of flow is from left to right

flow rate reduces the anoxic volume of the column, leading to a reduction in the total denitrification rate. The fact that this occurred within such a narrow flow range, however, suggests that this phenomenon is of limited importance in real environmental systems where flow rates have been reported to range from ~4 to 130 cm h^{-1} in the surface of sediments with topography-induced flushing rates (Precht & Huettel 2004).

The flow-through chamber optode experiment provided further evidence to suggest that anoxic niche formation within the sediment had a limited effect on denitrification. In agreement with the previous work of Franke et al. (2006), we observed a plume of low oxygen porewater downstream of the *Ulva lactuca*. The formation of this plume is most likely caused by microbial consumption of oxygen as leached dissolved organic carbon from *U. lactuca* is degraded (Franke et al. 2006). There was no formation of a flow dead zone behind the *U. lactuca* as illustrated by the dye experiments (Fig. 3) and the optode experiments, which clearly shows a minimal impact of the *U. lactuca* on porewater O_2 concentration before it started to degrade (Fig. 4a). This highlights the importance of dispersion in mixing solutes at this spatial scale within permeable sediments.

For denitrification to occur within this plume, it must become completely anoxic (Evrard et al. 2013). Whether or not the plume becomes anoxic is an interaction between flow velocity and the microbial respiration rate within the sediment and the macroalgae and associated plume. As the microbial community became established within the DOC plume from the macroalgae, it became increasingly anoxic at a given flow velocity (Fig. 4). At high flow velocities, the plume was oxic, and denitrification rates were very low (Figs. 5 & 6). At a flow velocity of 12.3 cm h^{-1} in E3, we were able to create an anoxic region within the sediment surrounded by hypoxic porewater. Under these conditions, the rate of denitrification was measured to be only 3 µmol m^{-2} h^{-1} within the column. Under low flow settings, the presence of macroalgae did increase the anoxic region of the sediment (Fig. 5); however, it was only once the column became anoxic

across its entire width (i.e. the outflow became anoxic) that denitrification rates increased substantially (Fig. 6). This suggests that the rate of lateral mixing (parallel to the axis of flow) of NO_3^- into the anoxic plume is limited, and it is only when there is a direct pumping of NO_3^- into the anoxic zone (perpendicular to the axis of flow) that rates increase substantially. The point at which this occurs depends most strongly on the bulk sediment oxygen consumption rate, rather than the presence of macroalgal detritus. These results show that whilst there is a rapid onset of denitrification within the anoxic niches, their volumetric extent limits significant rates of denitrification taking place.

Our inability to detect anoxic microzones both directly with planar optode and indirectly via enhanced denitrification has broader implications for our understanding of denitrification within permeable sediments. Previous studies have reported significant rates of denitrification within otherwise aerobic column experiments, and one explanation for this is that denitrification takes place within anoxic microniches (Rao et al. 2008, Santos et al. 2012). Even with cm-scale pieces of highly labile material we were unable to induce anoxic zones within an otherwise oxic sediment. The circumstances under which anoxic microniches are likely to occur within permeable sediments are therefore likely to be highly specific, requiring relatively large (cm-scale) pieces of labile material within a permeable matrix that itself has a low metabolic rate. Another possible scenario is that microsites occur within a zone of reduced transport owing to low porosity, such as within carbonate sand grains. Under this scenario, however, the transport of NO_3^- into the anoxic zone is also likely to be limited, so the extent to which this type of anoxic microzone would enhance denitrification remains unknown. We suggest that the precise conditions under which anoxic microsites are likely to occur be explored using reactive transport modeling, which is being used to provide many insights into the interactions between flow and biogeochemistry in permeable sediments (Meysman et al. 2007).

Flume experiments

The flume tank experiments show that the porewater flow dynamics (and subsequently denitrification rates) were highly dependent upon the placement of the *Ulva lactuca* relative to sediment ripple geometry. If the obstruction was placed midway between the ripple trough and peak, a plume of reduced oxygen concentration could be observed downstream, similar to that observed in the planar optode column experiments (Fig. 7). Additionally, the obstructed ripples exhibited substantially deeper oxygen penetration compared with the control ripples. In contrast, in Expt F2 the obstruction was placed at the base of the trough and no plume of lower oxygen concentration was observed, and there was no difference in the oxygen penetration dynamics between the obstructed and control ripples. The deeper oxygen penetration observed in Expt F1 appears to arise from a deflection effect brought about by the obstruction positioned perpendicular to the point at which there is the maximum flow velocity of porewater into the sediment. Along with dissolved oxygen, other solutes such as nitrate and denitrified N_2 will be channeled deeper into the sediment — which is illustrated for isotopically labeled N_2 in Fig. S1 in the Supplement, and conceptually in Fig. 8.

This data suggests if an obstruction is placed at the maximum point of porewater advection, a hydrodynamic effect can arise which can serve to channel porewater deeper into the sediment, where elevated rates of denitrification may arise. However, the layering and orientation of the *Ulva lactuca* sheets that was implemented during this experiment is unlikely to occur *in situ,* so the elevated denitrification rates observed should be considered a highly unlikely consequence of buried macroalgae being present in permeable sands.

Environmental relevance

Extrapolating the results of this study to environmental relevance is difficult. Even though we used

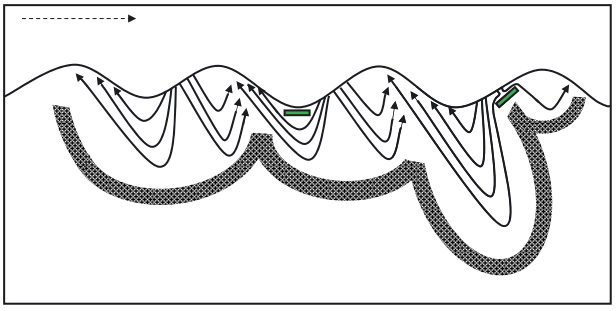

Fig. 8. Conceptual model comparing the influence of the position of the buried *Ulva lactuca* (small green rectangles) relative to ripple geometry on porewater advection. Solid arrows represent direction of porewater advection and dark hashed area represents anoxic sediment where denitrification is likely to occur. Dashed arrow indicates the flow direction of the overlying water

2 contrasting experimental designs with highly controlled porewater flow fields as well as more realistic flow fields in the flume, there are an infinite range of *Ulva lactuca* sheet sizes, densities and spatial distributions that we could have used. The size chosen here reflects a pragmatic need to be able to undertake lab experiments at a reasonable scale, and what we believed *a priori* to represent a minimum size required to induce anoxia. The experiments undertaken suggest that pieces of *Ulva lactuca* with a size of ~1 cm^2 are the minimum required to induce anoxia within highly flushed permeable sediment. As discussed above, the critical factor determining the denitrification rate is the bulk porewater oxygen consumption rate. Many small pieces of macroalgae within the sediment would have the effect of increasing the bulk porewater respiration rate, and hence increase the potential sediment denitrification rate. It will, however, also reduce the sediment nitrification rate — which is likely to be a critical limiting step in denitrification within the flow fields of permeable sediments (Kessler et al. 2012). Increasing the sheet size would result in larger zones of anoxia, but as shown in the flume experiment, this would start to deflect flow fields significantly. We speculate that the anoxic zones formed behind such large sheets will have a limited solute transport into them owing to the flow field deflection effect. Given that the rate of denitrification is controlled by the rate of NO_3^- transport into the anoxic zone of the sediment, it seems unlikely that significant denitrification will occur within such an anoxic zone. We therefore suggest that the main mechanism by which buried *U. lactuca* stimulates denitrification is through the release of NH_4^+ into the sediment, which is first nitrified then denitrified elsewhere in the sediment. Our data therefore suggest that nitrogen from remineralised macroalgae will be efficiently returned to the water column in permeable sediment environments, in agreement with previous studies (Trimmer et al. 2000, McGlathery et al. 2007).

Acknowledgements. We thank R. Glud and M. Larsen for assistance setting up the planar optodes and thoughtful comments on this work. We thank V. Evrard for skillfully undertaking the isotope analyses. This work was supported by the Australian Research Council grant DP1096457.

LITERATURE CITED

Boudreau BP, Huettel M, Forster S, Jahnke RA and others (2001) Permeable marine sediments: overturning an old paradigm. EOS Trans Am Geophys Union 82:133–136

Cardenas MB, Cook PLM, Jiang HS, Traykovski P (2008) Constraining denitrification in permeable wave-influenced marine sediment using linked hydrodynamic and biogeochemical modeling. Earth Planet Sci Lett 275: 127–137

Conley DJ, Paerl HW, Howarth RW, Boesch DF and others (2009) Controlling eutrophication: nitrogen and phosphorus. Science 323:1014–1015

Cook PLM, Røy H (2006) Advective relief of CO_2 limitation in highly productive sandy sediments. Limnol Oceanogr 51:1594–1601

Cook PLM, Wenzhöfer F, Rysgaard S, Galaktionov OS and others (2006) Quantification of denitrification in permeable sediments: insights from a two-dimensional simulation analysis and experimental data. Limnol Oceanogr Methods 4:294–307

Dalsgaard T (2003) Benthic primary production and nutrient cycling in sediments with benthic microalgae and transient accumulation of macroalgae. Limnol Oceanogr 48: 2138–2150

Emery KO (1968) Relict sediments on continental shelves of the world. Am Assoc Pet Geol Bull 52:445–464

Evrard V, Glud RN, Cook PLM (2013) The kinetics of denitrification in permeable sediments. Biogeochemistry 113: 563–572

Eyre BD, Ferguson AJP (2009) Denitrification efficiency for defining critical loads of carbon in shallow coastal ecosystems. Hydrobiologia 629:137–146

Eyre BD, Maher D, Oakes JM, Erler DV, Glasby TM (2011) Differences in benthic metabolism, nutrient fluxes, and denitrification in *Caulerpa taxifolia* communities compared to uninvaded bare sediment and seagrass (*Zostera capricorni*) habitats. Limnol Oceanogr 56:1737–1750

Franke U, Polerecky L, Precht E, Huettel M (2006) Wave tank study of particulate organic matter degradation in permeable sediments. Limnol Oceanogr 51:1084–1096

Gihring TM, Canion A, Riggs A, Huettel M, Kostka JE (2010) Denitrification in shallow, sublittoral Gulf of Mexico permeable sediments. Limnol Oceanogr 55:43–54

Guinda X, Juanes JA, Puente A, Echavarri-Erasun B (2012) Spatial distribution pattern analysis of subtidal macroalgae assemblages by a non-destructive rapid assessment method. J Sea Res 67:34–43

Hardison AK, Canuel EA, Anderson IC, Veuger B (2010) Fate of macroalgae in benthic systems: carbon and nitrogen cycling within the microbial community. Mar Ecol Prog Ser 414:41–55

Huettel M, Roy H, Precht E, Ehrenhauss S (2003) Hydrodynamical impact on biogeochemical processes in aquatic sediments. Hydrobiologia 494:231–236

Kessler AJ, Glud RN, Cardenas MB, Larsen M, Bourke M, Cook PLM (2012) Quantifying denitrification in rippled permeable sands through combined flume experiments and modelling. Limnol Oceanogr 57:1217–1232

Larsen M, Borisov S, Grunwald B, Klimant I, Glud RN (2011) A simple and inexpensive high resolution color ratiometric planar optode imaging approach: application to oxygen and pH sensing. Limnol Oceanogr Methods 9: 348–360

McGlathery KJ, Sundback K, Anderson IC (2007) Eutrophication in shallow coastal bays and lagoons: the role of plants in the coastal filter. Mar Ecol Prog Ser 348:1–18

McMillan SK, Piehler MF, Thompson SP, Paerl HW (2010) Denitrification of nitrogen released from senescing algal biomass in coastal agricultural headwater streams. J Environ Qual 39:274–281

Meysman FJR, Galaktionov OS, Cook PLM, Janssen F,

Huettel M, Middelburg JJ (2007) Quantifying biologically and physically induced flow and tracer dynamics in permeable sediments. Biogeosciences 4:627–646

Nielsen LP (1992) Denitrification in sediment determined from nitrogen isotope pairing. FEMS Microbiol Ecol 86: 357–362

Precht E, Huettel M (2004) Rapid wave-driven advective pore water exchange in a permeable coastal sediment. J Sea Res 51:93–107

Precht E, Franke U, Polerecky L, Huettel M (2004) Oxygen dynamics in permeable sediments with wave-driven porewater exchange. Limnol Oceanogr 49:693–705

Rao AMF, McCarthy MJ, Gardner WS, Jahnke RA (2008) Respiration and denitrification in permeable continental shelf deposits on the South Atlantic Bight: N_2: Ar and isotope pairing measurements in sediment column experiments. Cont Shelf Res 28:602–613

Reynolds WD (2008) Saturated hydraulic properties: laboratory methods. In: Carter MR, Gregorich EG (eds) Soil sampling and method of analysis, 2nd edn. CRC Press, Boca Raton, FL, p 1013–1024

Santos IR, Eyre BD, Glud RN (2012) Influence of porewater advection on denitrification in carbonate sands: evidence from repacked sediment column experiments. Geochim Cosmochim Acta 96:247–258

Seitzinger SP, Giblin AE (1996) Estimating denitrification in North Atlantic continental shelf sediments. Biogeochemistry 35:235–260

Tabarsa M, Rezaei M, Ramezanpour Z, Waaland JR (2012) Chemical compositions of the marine algae *Gracilaria salicornia* (Rhodophyta) and *Ulva lactuca* (Chlorophyta) as a potential food source. J Sci Food Agric 92: 2500–2506

Trimmer M, Nedwell DB, Sivyer DB, Malcolm SJ (2000) Seasonal organic mineralisation and denitrification in intertidal sediments and their relationship to the abundance of *Enteromorpha* sp. and *Ulva* sp. Mar Ecol Prog Ser 203: 67–80

Editorial responsibility: Erik Kristensen, Odense, Denmark

Submitted: May 23, 2013; Accepted: October 17, 2013
Proofs received from author(s): January 20, 2014